

## INFLUENCE OF SYNTHESIS PARAMETERS IN THE PREPARATION OF SILICON (IV) OXIDE NANOPARTICLES FROM DEALUMINATED METAKAOLIN AND METAKAOLIN WITH $\text{Na}_2\text{SiO}_3$

J.O. Tijani<sup>1,3</sup>, M.T. Bankole<sup>1,3</sup>, A. Hussein<sup>1</sup>, J.A. Oketoye<sup>1</sup> and A.S. Abdulkareem<sup>2,3</sup>

<sup>1</sup>Department of Chemistry, Federal University of Technology, PMB. 65, Minna, Niger State

<sup>2</sup>Department of Chemical Engineering, Federal University of Technology, PMB.65, Minna, Niger State, Nigeria

<sup>3</sup>Nanotechnology Research Group, Centre for Genetic Engineering and Biotechnology (CGEB), Federal University of Technology, P.M.B 65, Bosso, Minna, Niger State, Nigeria

\*Corresponding author: [jimohtijani@futminna.edu.ng](mailto:jimohtijani@futminna.edu.ng), +2348057344464

Received 19 August 2019; accepted 23 September 2019, published online 25 October 2019

### Abstract

$\text{SiO}_2$  nanoparticle is a versatile material with diverse technological applications. However, the cost associated with the production from chemical and biological source is high and the quantity or yield produced is often small which cannot adequately meet the increasing demands of the population. Thus, there is need to prepare  $\text{SiO}_2$  nanoparticle from readily available material like kaolin. In this research work,  $\text{SiO}_2$  nanoparticles was synthesized from dealuminated metakaolin and metakaolin with  $\text{Na}_2\text{SiO}_3$  at different solution pH (5, 8 and 10), concentration of NaOH (0.5 M, 1 M and 2 M), calcination temperatures (600°C, 700°C and 800°C). The prepared  $\text{SiO}_2$  nanoparticles was characterized by X-ray Diffraction (XRD), High Resolution Scanning Electron Microscope (HRSEM), and Energy Dispersive Spectroscopy (EDS). The XRD analysis demonstrated that  $\text{SiO}_2$  nanoparticle produced at calcination temperatures of 600°C and 800°C from dealuminated metakaolin and metakaolin with  $\text{Na}_2\text{SiO}_3$  at 700°C and 800°C were highly and purely crystalline. While the optimum concentration of NaOH and pH to prepare pure  $\text{SiO}_2$  nanoparticles from dealuminated metakaolin was 0.5 M and pH 8 respectively. The HRSEM analysis revealed morphological transformation from slate to rod-like, compacted trigonal to spherical structures depending on the applied synthesis conditions. EDS analysis revealed high amount of Si and O at the optimum synthesis conditions for both metakaolin with  $\text{Na}_2\text{SiO}_3$  and dealuminated metakaolin except for  $\text{SiO}_2$  nanoparticles prepared at other conditions which contained impurities. Of all the two sources considered, the study demonstrated that highly crystalline and pure  $\text{SiO}_2$  nanoparticle could be synthesized from dealuminated metakaolin via hydrothermal route.

**Keywords:**  $\text{SiO}_2$  nanoparticles, metakaolin, dealuminated kaolin, hydrothermal method,

### INTRODUCTION

Silica is an inorganic oxide formed via polymerization of certain organic minerals [1]. It is considered as one of the most abundant minerals on the earth and very useful for a wide range of industrial applications such as adsorbent, catalyst and catalyst support [2]. Furthermore, silica can be used for the production of ceramic, cement, concrete, insulator, optical, electronic composite materials and water glass desiccant [3].  $\text{SiO}_2$  is bound to

four oxygen atom with each oxygen bonded to two silica atom [3]. The high Si – O – Si angle is often responsible for the large number of silica polymorphs ranging from crystalline and amorphous structure, non-periodic porous system to regular structural pattern and microporous crystalline system [4].  $\text{SiO}_2$  often possessed high activity and stability which enhanced selectivity, metal tolerance and flexibility when used as an additive catalyst [6].

In addition, silica is used as the raw materials for the production of water glass desiccant [3]. Silica and inorganic template such as tetraethylorthosilicate (TEOS) are usually employed for the synthesis of zeolites and other mesoporous material. The preparation of SiO<sub>2</sub> is usually done via a hydrothermal treatment of alumina and metasilicate in the presence of organic template [7]. The use of toxic chemicals in the synthesis of SiO<sub>2</sub> caused environmental pollution and this is the major reason why SiO<sub>2</sub> should be synthesized from naturally available material. Several research efforts have focused on the synthesis of silica from rice husk ash (RHA) and microorganisms. The biological material is considerably limited in terms of availability and hence cannot meet the increasing demands of SiO<sub>2</sub> nanoparticles for industrial applications. Not only that, the existing chemical methods of preparing SiO<sub>2</sub> nanoparticles complex and are energy intensive. For instance, [8] have utilized the fungus *Fusarium oxysporum* to transform the natural occurring amorphous bio-silica in rice husk into quasi-spherical shaped, highly crystalline silica nanoparticle (quartz) of 2 – 6 nm diameter. [9], also attempted the synthesis of silica body like structure artificial organs; bone repair scaffolds drug vectors and holographic systems to form a composite of biological polymers and silicon. The authors were of the opinion that biological method of producing nano sized silica consumed time on the other hand conserves energy [1]. In view of this, the development of new material which possesses a super-size reduction dimension for enhanced technological advancement by scientists and researchers is still ongoing [10]. One of the naturally available materials often used to prepare metallic oxide nanoparticle is Kaolin. Kaolin clay or white clay are rich in mineral called kaolinite and are categorized as layered silicate mineral [11]. The dehydroxylation process of raw kaolin in the furnace often transformed the kaolin particle to metakaolin [12]. Metakaolin is ordinarily used in ceramics industries and also as a construction material. Metakaolin has an excellent resistance to water which aid reinforcement of the mechanical properties of concrete in construction industry application. Metakaolin in concrete applications reduces the water

penetration and alkali silica reaction by acting as filter thereby increases hydration process [1]. The major constituents of metakaolin include alumina (Al<sub>2</sub>O<sub>3</sub>), silica otherwise known as SiO<sub>2</sub>, and trace amount of FeO, ZnO, and TiO<sub>2</sub>. The extraction of silica from kaolin or metakaolin proceeds in series of processes that involve clay preparation, heat treatment and use of sodium hydroxide as agent for extraction [13]. However, reaction time, solution pH, concentration of NaOH for the removal of silica is crucial to its yield. There is limited information in the literature on the optimization of the preparation parameters such as calcination temperature, solution pH, concentration of NaOH, stirring speed, reaction time on the purity and yield of SiO<sub>2</sub> from natural sources such as kaolin or metakaolin. Therefore, this study focused on the influence of NaOH, calcinations temperature and solution pH on the purity and phase type of SiO<sub>2</sub> nanoparticle obtained from dealuminated metakaolin and metakaolin with Na<sub>2</sub>SiO<sub>3</sub>.

## MATERIALS AND METHODS

The following analytical grade chemicals/reagents used in this study namely sodium hydroxide, tetraoxosulphate (VI) acid, sodium metasilicate with percentage purity in the range 96-99% were obtained from Sigma Aldrich. The chemicals were used without further purification.

### Sample collection and pretreatment of kaolin

The raw kaolin obtained from Ahoko, Kogi State was crushed to powder form using mortar and pestle. Thereafter, 20 g of the powdered sample was weighed into a crucible and subsequently calcined in the furnace at a temperature of 600°C for 6 h to reduce the moisture content. The calcination process transformed the kaolin to metakaolin.

### Dealumination of metakaolin

The procedure for the dealumination of metakaolin can be described as follow; 50 g of metakaolin was mixed with 150 cm<sup>3</sup> of deionized water to form a homogenous mixture in a 250 cm<sup>3</sup> conical flask. After which, 100 cm<sup>3</sup> of 98 Wt% H<sub>2</sub>SO<sub>4</sub> was added to the mixture

and shaken vigorously for 6 h on a magnetic stirrer at stirring speed of 1000 rpm to prevent the content from forming mud. The mixture was later left to age without external heating for about 3 h and then washed with deionized water, filtered and oven dried at 120°C for 2 h [12].

#### **Synthesis of Silicon Dioxide nanoparticles using dealuminated metakaolin at different pH, calcination temperature and NaOH concentration**

The synthesis was done by measuring 100 cm<sup>3</sup> of the deionized water into 250 cm<sup>3</sup> conical flasks followed by dissolution of 1.2 g of dealuminated metakaolin and 1 g NaOH. The mixture was stirred on a magnetic stirrer at 1000 rpm for 6 h and 1M H<sub>2</sub>SO<sub>4</sub> and 1M NaOH was added to adjust the pH to the desired pH value of 5, 8 and 10. Once the desired pH was achieved, the mixture was stirred at different pH for 6 h and allowed to age for 12 h. The hydrothermal process was carried out at 200°C for 6 h using an autoclave reactor (Teflon). After the crystallization, the sample was washed in distilled water until it reaches pH of 7 (neutral) and allow to age. The sample obtained at different pH values was then subjected to calcination process at different temperature of 600°C, 700°C, 800°C and crystallization time of 8 h each. The procedure was repeated using optimum pH and calcination temperature to prepare SiO<sub>2</sub> nanoparticles at different concentration of NaOH (0.5 M, 1 M and 2 M).

#### **Synthesis of SiO<sub>2</sub> Nanoparticle from mixture of metakaolin and Na<sub>2</sub>SiO<sub>3</sub> at different pH, calcination temperature and NaOH concentration**

SiO<sub>2</sub> nanoparticle was synthesized using metakaolin without organic template. The synthesis was done by measuring 100 cm<sup>3</sup> of the deionized water into a 500 cm<sup>3</sup> beaker followed the dissolution of 1 g of NaOH, 1.2 g of powdered metakaolin and 22.83 g of Na<sub>2</sub>SiO<sub>3</sub> was added and the mixture was stirred for 6 h and later allowed to age for 12 h. The whole mixture was then dissolved in NaOH solution at different concentrations (0.5 M, 1 M and 2 M) and stirred on a magnetic stirrer at 500 rpm for 6

h and later allowed to age overnight. The aged sample was put inside an autoclave Teflon reactor for hydrothermal process at 200°C for 6 h. After the crystallization, SiO<sub>2</sub> nanoparticle was washed with distilled water until it reaches pH of 7 (neutral) and allow to age. The crystal obtained was then subjected to calcination in the furnace at different temperature of 600°C, 700°C, 800°C and crystallization time of 8 h each. This procedure was repeated under the optimum concentration of NaOH, crystallization temperature but different solution pH (5, 8 and 10).

#### **Characterization of the prepared materials**

High Resolution Scanning Electron Microscope (HRSEM) coupled with Energy Dispersive X-ray Spectroscopy (EDS) (Zeiss Auriga model) was utilized to examine the surface morphology and elemental composition under the following measurement operating conditions: electron high tension (EHT) 5 Kv, current 10 Ma, Aperture (0.4 mm), magnification varies. For the EDS, the detector angle was 150°. The phase structure of the materials were examined using Bruker D8 X-ray Diffractometer operated at the following conditions, scanning angle range (20-90°), scanning speed and step (60s/step, 0.2°), operating current and voltage (40 mA, 40 kV).

## **RESULTS AND DISCUSSION**

### **High Resolution Scanning Electron Microscopy Analysis of the Prepared Samples**

The surface morphology of the SiO<sub>2</sub> nanoparticle prepared from the dealuminated metakaolin at different synthesis conditions were examined using HRSEM and the results are shown in Figure 1 - 3 respectively by HRSEM and the results was shown in Figure 1-3.

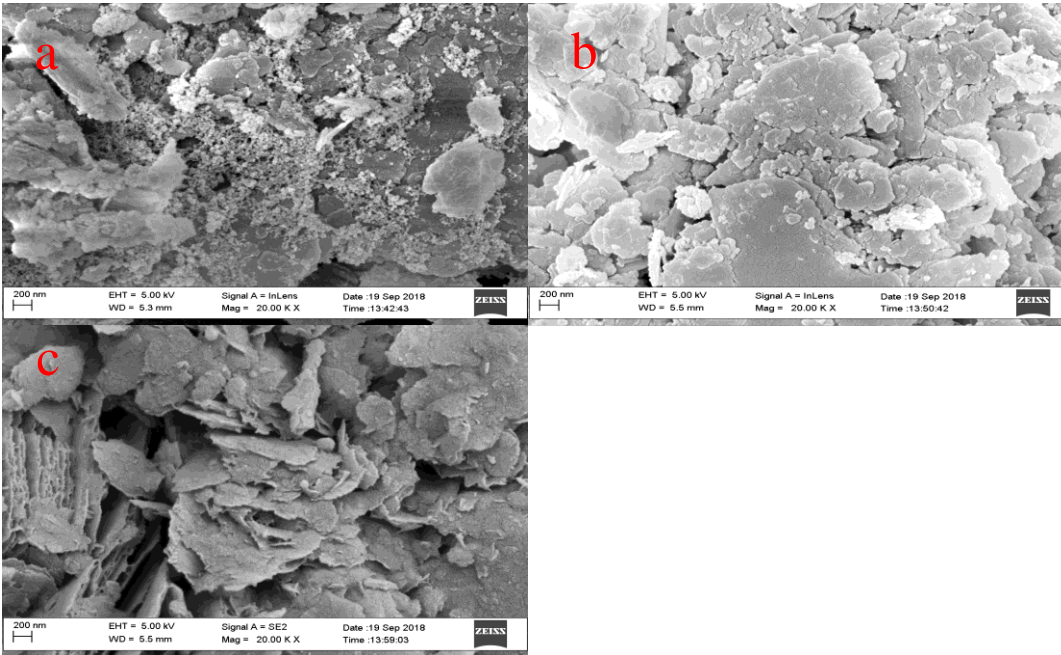


**Figure 1: HRSEM micrograph of SiO<sub>2</sub> nanoparticles prepared from dealuminated metakaolin at different temperatures (a) 600°C (b) 700°C (c) 800°C**

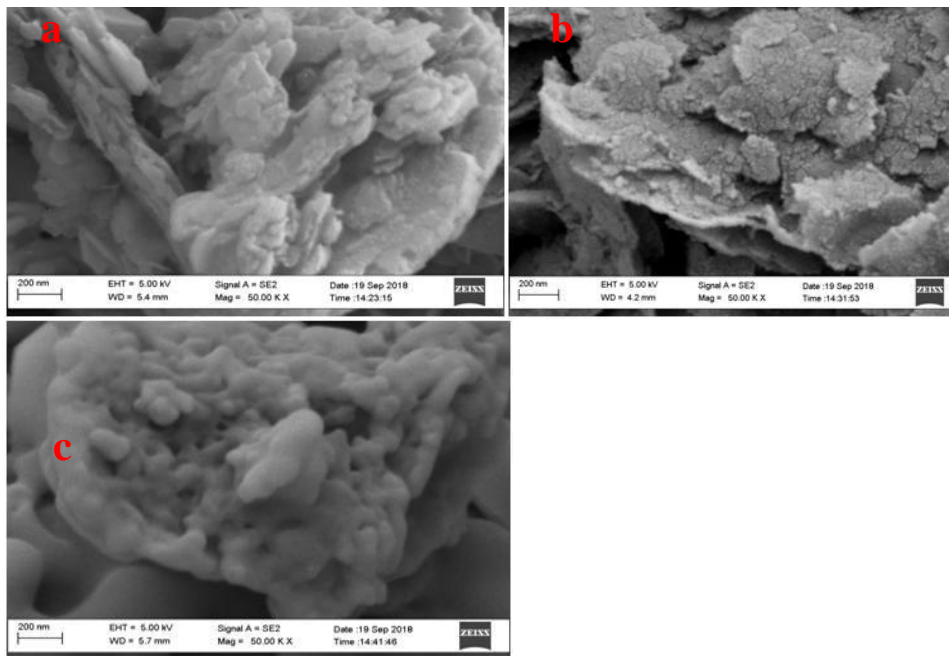


**Figure 2: HRSEM micrograph of SiO<sub>2</sub> nanoparticles prepared from dealuminated metakaolin at different pH (a) 5 (b) 8 (c) 10**

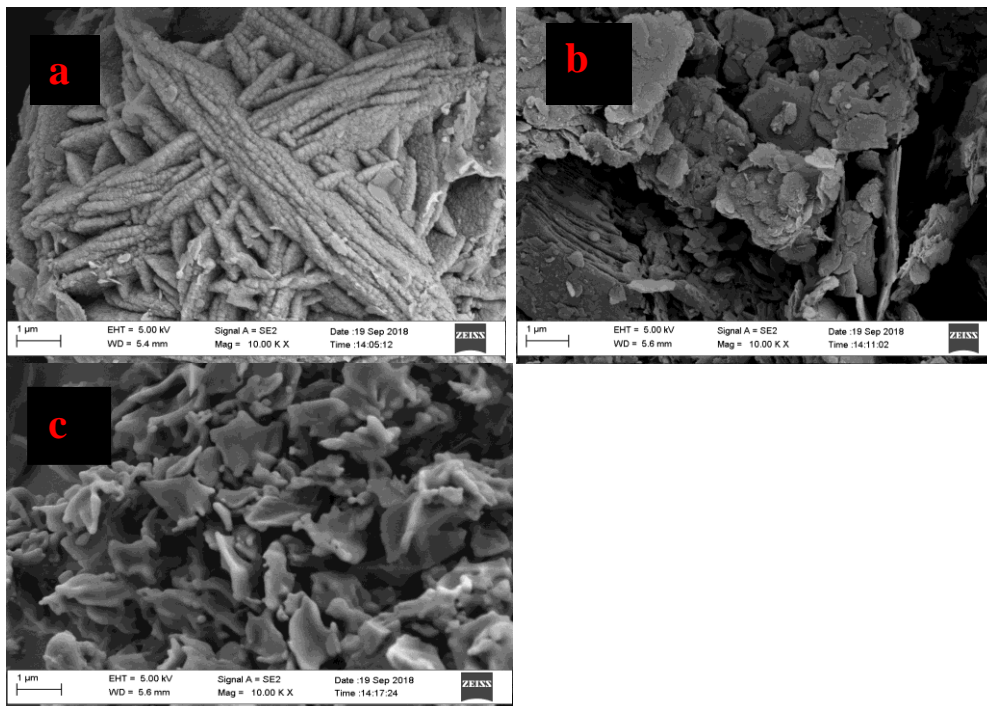


**Figure 3: HRSEM micrographs of SiO<sub>2</sub> nanoparticles prepared from dealuminated metakaolin different concentration of NaOH (a) 0.5 M (b) 1M (c) 2M**

Figure 1 (a) showed the presence of highly dispersed, irregular and scattered grain of slate like morphology irrespective of the calcinations temperature. However, a more compacted plate like structure was prominent at 700°C compared to other temperatures. While in Figure 2 (a), mixture of flaky layer and slate like morphology were observed. Figure 2 (b) revealed aggregated spherical structure and Figure 2 (c) demonstrated the formation of a trigonal thin spongy like and yet agglomerated structure suggesting phase transition from  $\alpha$ -Quartz to  $\beta$ -Quartz of the SiO<sub>2</sub> nanoparticle owing to increment in calcinations temperature. Figure 3 (a) demonstrated highly compacted thick and thin rod like network structure which possibly accounted for the mixed phase of the SiO<sub>2</sub> nanoparticle produced. The addition of NaOH caused strong attraction of the positively and negatively charged species in the dealuminated metakaolin particles to form large aggregates of flocs of different phases as noticed in (Fig 3 (a) to (c)). HRSEM micrograph (Figure 3 (b)) indicated the formation of mixture of spherical and slate like structure. In the case of Figure 3 (c), highly amorphous structure was formed

without any definite shape. The HRSEM results obtained further corroborated the XRD analysis shown in Figure 4 which revealed the formation of a mixed phase except for SiO<sub>2</sub> nanoparticles prepared from dealuminated metakaolin at solution pH 5 and calcinations temperature 700°C. This however contradicts the result reported by [14] who obtained only amorphous form of SiO<sub>2</sub> nanostructured prepared via sol-gel method. The differences may be linked to the different synthesis protocol employed.

#### **Energy Dispersive Spectroscopy (EDS) analysis of SiO<sub>2</sub> Nanoparticles**

The result of the elemental composition of the SiO<sub>2</sub> nanoparticle produced from dealuminated metakaolin prepared at different solution pH, calcination temperatures and concentration of NaOH determined by EDS is displayed in Table 1. According to Table 1, it can be noticed that the major elements in the synthesized materials are Si and O, which confirmed that the material produced was SiO<sub>2</sub> nanoparticles. Other elements such as Al, O, Fe, Ti, K were detected in trace amount which probably emanated from the metakaolin

precursor. The element carbon identified in the sample originated from the carbon adhesive tape used for the analysis while Na introduced was from NaOH used during the syntheses. The average percentage composition in Table 1 revealed that the SiO<sub>2</sub> nanoparticle produced from the dealuminated metakaolin was 73.95% while that of SiO<sub>2</sub> nanoparticle synthesized from

dealuminated metakaolin/Na<sub>2</sub>SiO<sub>3</sub> was 74.00%. The higher content of elemental Si and O in the latter than the former may be due to the additional incorporation of Na<sub>2</sub>SiO<sub>3</sub>.

**Table 1: Elemental composition of the produced SiO<sub>2</sub> nanoparticles under the applied conditions**

Samples	Elements								
	Si	Al	Na	O	C	K	Ti	S	Fe
Content (%)									
<b>Temperatures</b>									
600°C	16.25	12.23	0.92	53.20	15.61	0.54	0.57		
700°C	22.81	18.10	1.13	49.42	5.70	0.98	0.89		
800°C	14.92	12.77	1.93	59.33	9.84	0.43			0.39
<b>NaOH concentration</b>									
0.5 M	22.93	3.23	3.62	59.03	10.96	0.11	0.11		
1.0 M	24.70	10.86	1.67	47.56	12.09	1.52	0.69		
2.0 M	25.36	3.58	3.43	45.72	17.91	0.49			3.28
<b>Solution pH</b>									
5	27.62	8.35	8.04	44.06	7.73	1.47	1.55		1.18
8	14.64	12.96	2.47	56.80	12.00	0.27	0.40		1.45
10	29.76	3.09	10.92	48.96	4.95			232	

**X-ray Diffraction analysis of SiO<sub>2</sub> Nanoparticle prepared from dealuminated metakaolin**

The XRD patterns of the SiO<sub>2</sub> nanoparticle obtained from dealuminated metakaolin

prepared at different experimental conditions: solution pH (5, 8, 10), calcinations temperatures (600°C, 700°C and 800°C), concentration of NaOH (0.5 M, 1.0 M and 2.0 M) is displayed in Figure 4 – 6. While the crystallite size of the synthesized SiO<sub>2</sub> nanoparticles was estimated using Scherrer equation.

$$D = \frac{k\lambda}{\beta \cos\theta}$$

Where D is the average crystallite size K is a constant which depend on the crystallite

shape,  $\theta$  is the Braggs angle,  $\beta$  is the intense angle obtained from the full half width maximum respectively

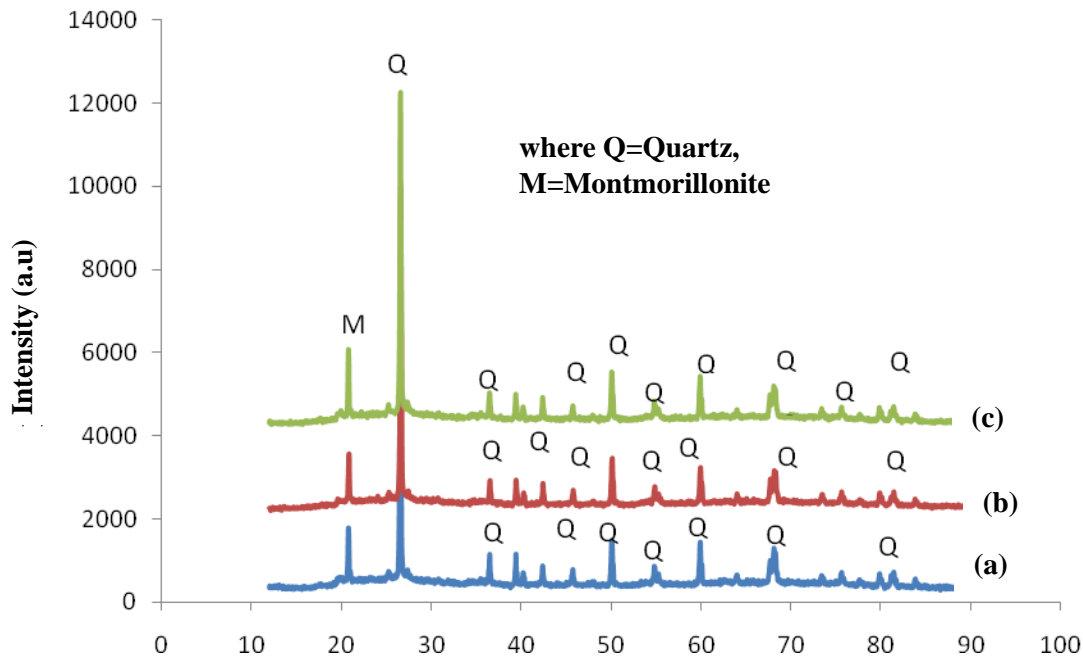


Figure 4: X-ray Diffraction of SiO<sub>2</sub> Nanoparticle from dealuminatedMetakaolincalcined at different temperatures (a) 600<sup>0</sup>C (b) 700<sup>0</sup>C and (c) 800<sup>0</sup>C for crystallization time of 8 h

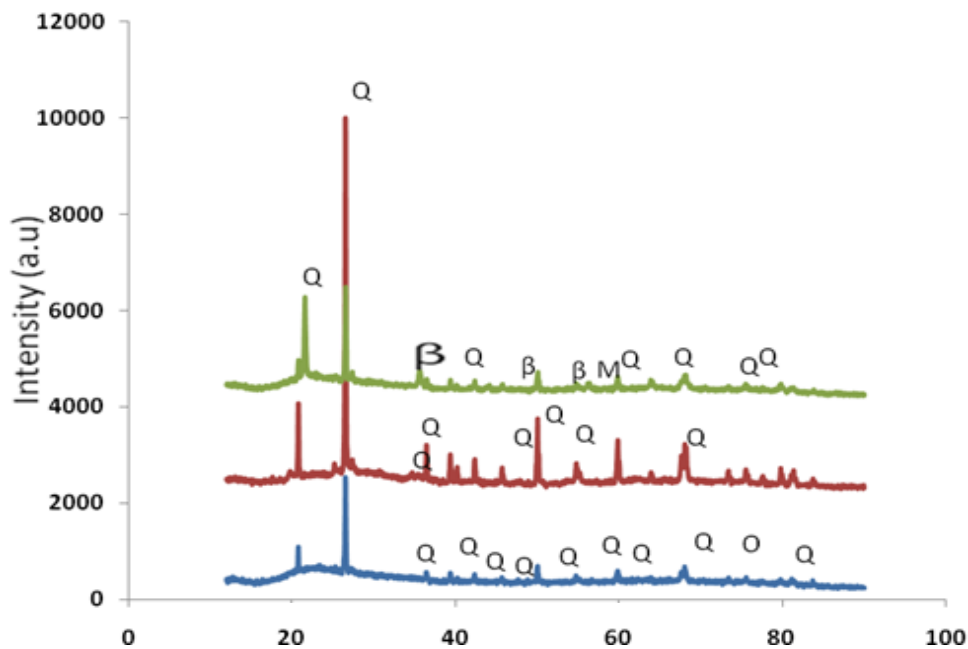
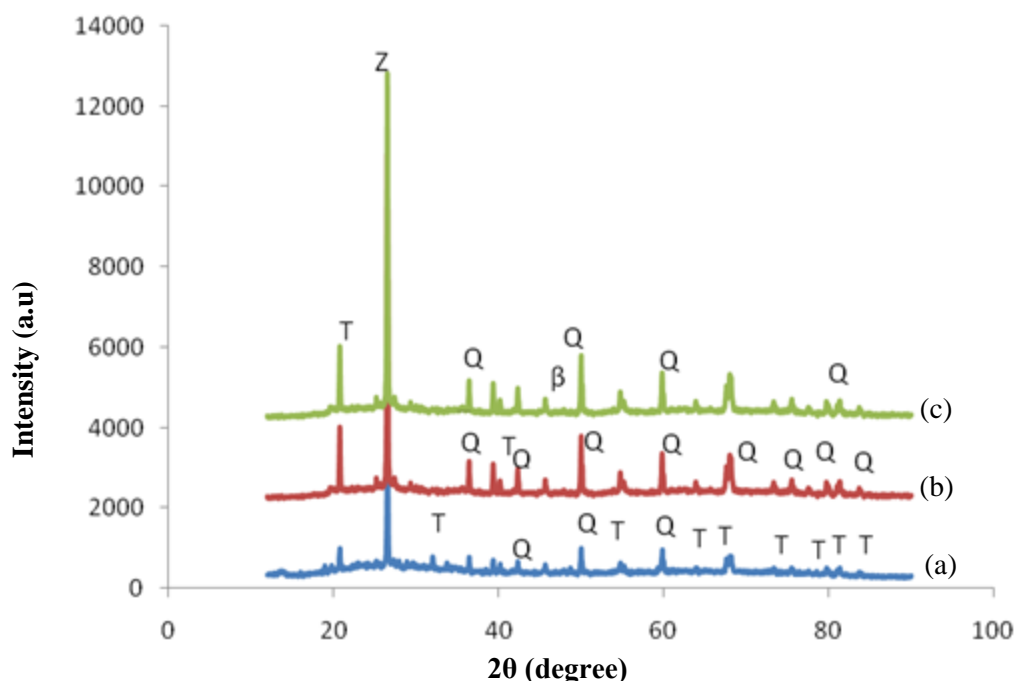


Figure 5: X-ray Diffraction of SiO<sub>2</sub> Nanoparticle prepared from DealuminatedMetakaolin at different pH (a) 5 (b) 8 (c) 10 (where Q=  $\alpha$ -Quartz, $\beta$ =  $\beta$ -Quartz M= Montmorillonite)



**Figure 6: X-ray Diffraction pattern of  $\text{SiO}_2$  Nanoparticle from Dealuminated Metakaolin at different concentration of NaOH (a) 0.5 M (b) 1 M (c) 2 M (Z=  $\alpha$ -Quartz+ $\beta$ -Quartz, T=Thermadite, Q=  $\alpha$ -Quartz,  $\beta$ =  $\beta$ -Quartz)**

Figure 4 revealed the formation of a mixed phase (mixture of Quartz and Montmorillonite) of  $\text{SiO}_2$  nanoparticles at different diffraction angles ( $2\theta$ ) values of  $20.28^\circ$ ,  $25.21^\circ$ ,  $39.37^\circ$ ,  $40.09^\circ$ ,  $50.04^\circ$ ,  $59.89^\circ$ ,  $68.08^\circ$ ,  $77.52^\circ$ ,  $78.92^\circ$ , respectively. These diffraction angles correspond to the following crystal planes (100), (100), (112), (211), (203), (220), (213) respectively. However diffraction angle observed at intensity of  $20.28^\circ$  corresponds to Montmorillonite phase. It was noticed that the intensity of the diffraction peak observed at  $2\theta$  of  $20.28^\circ$  increases with increasing temperature. The absence of broad peaks in the XRD pattern irrespective of the calcinations temperature suggests that the prepared material is highly crystalline in spite of its existence in two different phases. However, the peak intensities of the prepared material differ due to the differences in the applied conditions.

Figure 5 (a) also demonstrated the presence of diffraction peaks at  $2\theta$  values of  $20.78^\circ$ ,  $26.50^\circ$ ,  $37.23^\circ$ ,  $59.15^\circ$ ,  $40.71^\circ$ ,  $44.27^\circ$ ,  $53.20^\circ$ ,  $67.60^\circ$  corresponding to crystalline planes of (101), (110), (111), (200), (003) (101), (211) and (212) respectively. XRD pattern in Figure 5 (b)

revealed the presence of diffraction peaks at  $2\theta$  values of  $20.78^\circ$ ,  $26.50^\circ$ ,  $30.48^\circ$ ,  $36.45^\circ$ ,  $39.33^\circ$ ,  $45.65^\circ$ ,  $73.33^\circ$ ,  $75.87^\circ$ ,  $79.23^\circ$  and  $82.25^\circ$  which differ slightly from Figure 5 (a) with the following weak diffraction peaks at  $2\theta$  value of  $26.50^\circ$ ,  $30.48^\circ$ ,  $36.45^\circ$ ,  $37.65^\circ$ ,  $40.41^\circ$ ,  $66.19^\circ$ ,  $74.87^\circ$ ,  $78.68^\circ$  and  $82.76^\circ$ . These diffraction peaks were assigned the following crystal planes (100), (101), (202) (112), (203), (221), (300), (302), and (310). Figure 5 (c) indicated a mixture of alpha and beta quartz phase of  $\text{SiO}_2$  nanoparticles, which is completely different from the phases noticed in Figure 5 (a) and (b) respectively. The differences may be attributed to high alkaline nature of reaction mixture (pH 10) compared to weak alkaline (pH 8) and acidic nature (pH 5) of the  $\text{SiO}_2$  pattern shown in Figure 5 (a) and (b). In the case of Figure 5 (a) and (b), pure  $\text{SiO}_2$  nanoparticles were obtained even though the peaks intensities were low. On the other hand, a mixed phase ( $\alpha$  and  $\beta$  Quartz plus Montmorillonite) of  $\text{SiO}_2$  nanoparticle was shown in Figure 5 (c). The trend observed may be due to the differences in the applied temperature. The presence of sharp and intense diffraction peaks in Figure 5 (b) and (c) further account for the crystalline nature of



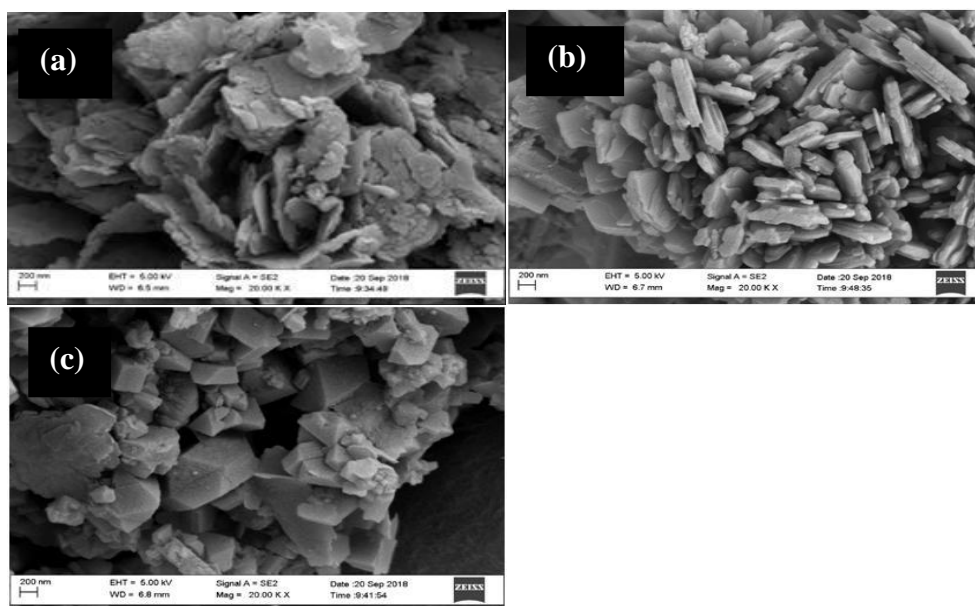
the SiO<sub>2</sub> nanoparticle compared to the Figure 5 (a).

Figure 6 (a) showed diffraction peaks pattern at  $2\theta$  values of 20.74°, 26.50°, 31.99°, 36.35°, 37.83°, 50.00°, 53.44°, 59.78°, 62.15°, 66.40°, 72.33°, 77.17°, 81.98°, with the following crystal planes of (111), (100), (212), (231), (311), (151), (110), (112) and (212), (371), (173), (424) (444) respectively. The most intense peaks at  $2\theta$  value of 20.74° and 26.50° indicated the existence of SiO<sub>2</sub> nanoparticles in different phases namely; thermadite,  $\alpha$ -quartz and  $\beta$ -quartz. The formation of mixed phases may be ascribed to the reaction of NaOH with the metal oxides in the dealuminated metakaolin. The detection of phases other than alpha quartz suggest the existence of impurities in the SiO<sub>2</sub> nanoparticles prepared at different concentration of NaOH even though the XRD analysis confirmed the formation of SiO<sub>2</sub> nanoparticles. None or absence of broad diffractions peaks implies large crystallite sizes and crystalline nature of the materials which differ slightly from the research work of [5] due to differences in experimental conditions. It can therefore be inferred that highly amorphous structure of SiO<sub>2</sub> was synthesized at calcination temperatures of 600°C and 800°C while crystalline SiO<sub>2</sub> nanoparticle was synthesized at calcination

temperature of 700°C. Furthermore, it was noticed that the crystallite size of SiO<sub>2</sub> nanoparticles calculated using Scherer equation increases with increasing calcinations temperature from 2.56 nm to 3.35 nm. In the case of solution pH, the crystallite size did not follow any specific trend. For instance at pH 5, the calculated crystallite size was 3.10 nm which however reduced to 2.39 nm at pH 8 and slightly increases to 4.25 nm at pH 10. The differences may suggest slow or fast homogeneous and heterogeneous nucleation at different applied pH. Similar trend was observed when the concentration of NaOH also varied from 0.5 M to 2.0 M.

#### HRSEM analysis of the prepared SiO<sub>2</sub> nanoparticles prepared from metakaolin mixed with Na<sub>2</sub>SiO<sub>3</sub>

HRSEM analysis of the prepared SiO<sub>2</sub> nanoparticles from metakaolin mixed with Na<sub>2</sub>SiO<sub>3</sub> at different calcinations temperatures, solution pH and concentration of NaOH was done to determine its morphology and microstructural properties. The HRSEM micrograph of the SiO<sub>2</sub> nanoparticles obtained under each synthesis conditions are shown in Figures 7 – 9 respectively.



**Figure 7: HRSEM micrograph of SiO<sub>2</sub> nanoparticles prepared from mixture of metakaolin and Na<sub>2</sub>SiO<sub>3</sub> at different temperatures (a) 600°C (b) 700°C (c) 800°C**

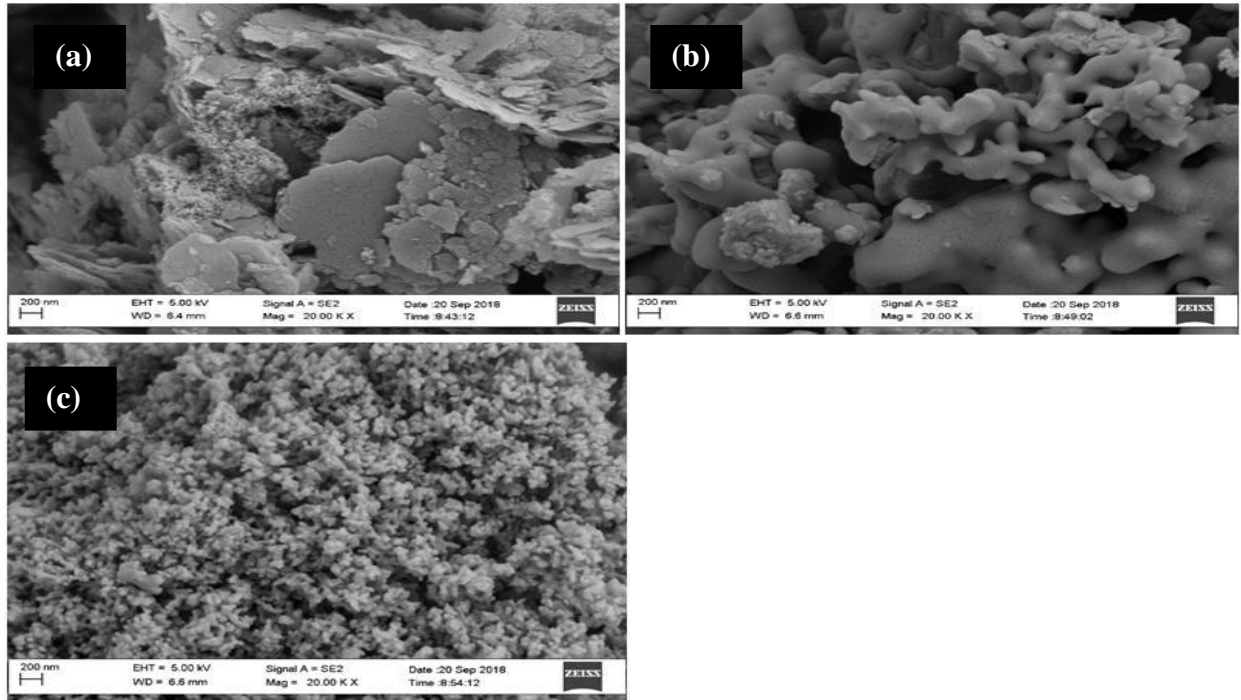


**Figure 8: HRSEM micrograph of SiO<sub>2</sub> nanoparticles prepared from mixture of metakaolin and Na<sub>2</sub>SiO<sub>3</sub> at different solution pH (a) 5 (b) 8 (c) 10**

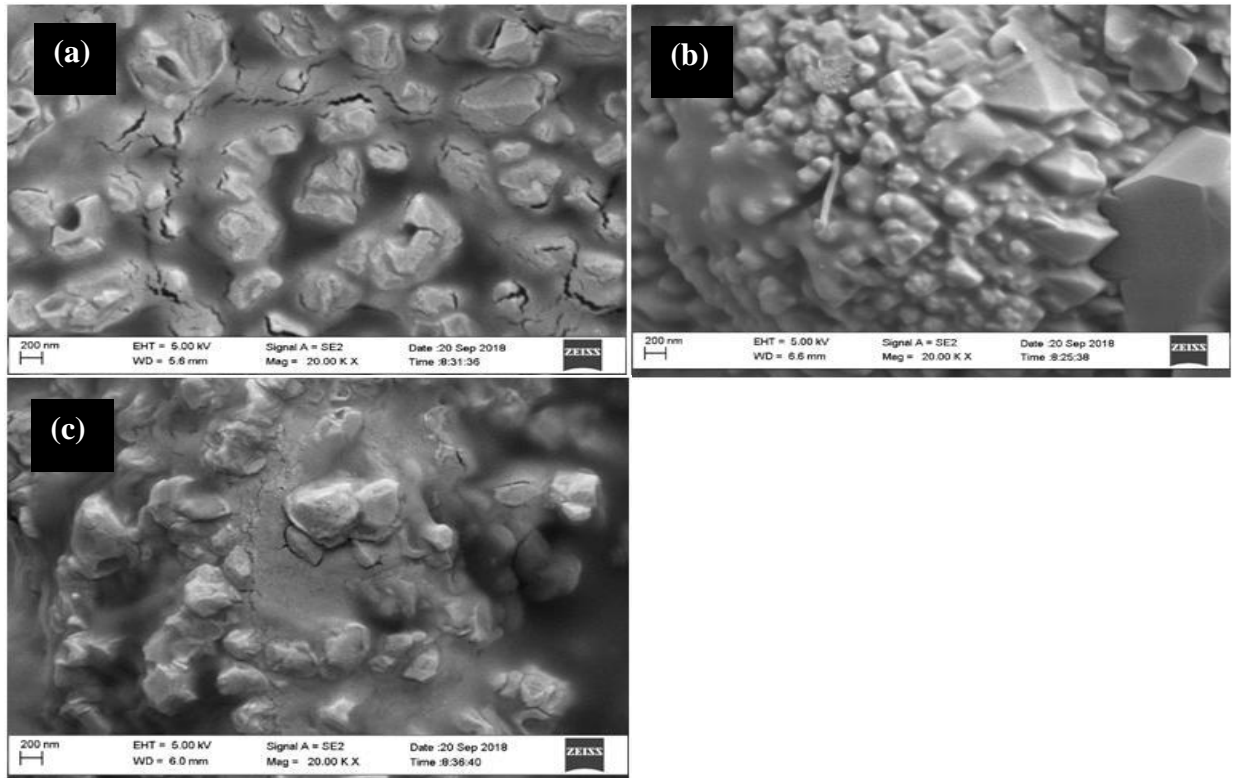


**Figure 9: HRSEM micrograph of SiO<sub>2</sub> nanoparticles prepared from mixture of metakaolin and Na<sub>2</sub>SiO<sub>3</sub> at different concentration of NaOH (a) 0.5 M (b) 1.0 M (c) 2.0 M**

Figure 7 (a) revealed the formation of plate like structure which gradually transformed to aggregated and compacted stack slate-like shape as the temperature was increased from 600-800°C. Very distinct and purely heterogeneous hexagonal shape SiO<sub>2</sub> nanoparticles were formed at 800°C (Figure 7 (c)). The morphological changes noticed may be linked to increase nucleation process caused by the increment in temperature. In addition, the plate-like morphology changed to soft and gum-like structure at pH 8. The adjustment of solution pH from 8 to 10 was also responsible for the formation of loosely homogeneous grains-like network. This further suggests that adjustment of the solution pH during the synthesis of SiO<sub>2</sub> nanoparticles largely determined the size and morphology of the final products. It was noticed that the SiO<sub>2</sub> crystals begun to form in Figure 9 (a) however the exact morphology could not be exactly defined. When the concentration of NaOH was increased to 1 M, agglomerated cubic shape particles were formed (Figure 9 (b)). In the same vein, when the concentration of NaOH was doubled compared to Figure 9 (b), more compacted hexagonal shape was noticed. The hexagonal morphology observed in Figure 9 (b) however disappeared when the concentration of NaOH was adjusted to 2.0 M and highly dispersed pyramidal rod-like shape was formed. This again implies that

addition of NaOH influenced the shape of the formed SiO<sub>2</sub> nanoparticles. Comparatively, the three investigated parameters influenced the morphology of prepared SiO<sub>2</sub> nanoparticles. The observed trend in this study closely agreed with the findings of [15], who synthesized SiO<sub>2</sub> nanostructures from Tetraethyl orthosilicate as a precursor, and found that the powders consist of fine particle that adhered to each other.

#### X-ray Diffraction analysis of the prepared SiO<sub>2</sub> nanoparticles from dealuminated metakaolin mixed with Na<sub>2</sub>SiO<sub>3</sub>

The mineralogical phase of the prepared SiO<sub>2</sub> nanoparticles from mixture of Na<sub>2</sub>SiO<sub>3</sub> and dealuminated kaolin at different concentration of NaOH, solution pH and calcinations temperatures was determined using XRD. The XRD pattern obtained under the applied conditions are shown in Figure 10 - 12 respectively while the grain size of the prepared SiO<sub>2</sub> nanoparticles was calculated using Scherrer's equation.

$$D = \frac{a\lambda}{\beta \cos\theta}$$

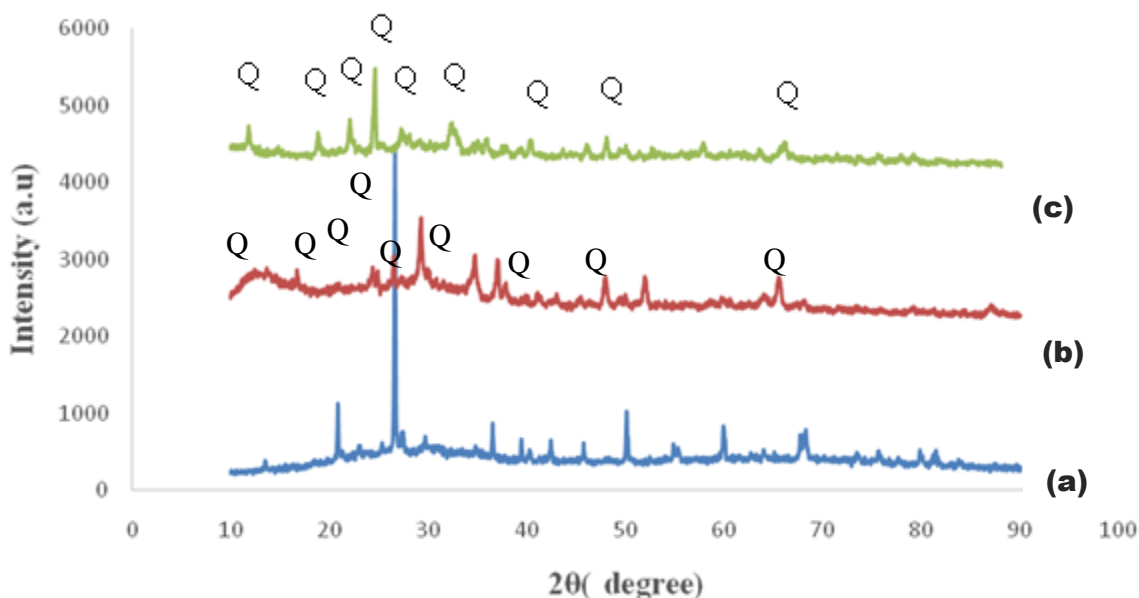


**Figure 10: X-ray Diffraction pattern of SiO<sub>2</sub> nanopartiles prepared from metakaolin with Na<sub>2</sub>SiO<sub>3</sub> at different concentration of NaOH (a) 0.5M, (b) 1M (c) 2M NaOH. (Where Q = Quartz)**

It can be noticed from Figure 10 (a – c) that only one phase of SiO<sub>2</sub> nanoparticles was produced from mixture of dealuminated metakaolin and Na<sub>2</sub>SiO<sub>3</sub> irrespective of the concentration of NaOH. The diffraction peaks observed at the 2θ value of 27.28°, 29.27°, 24.64° with the following crystal planes (101), (110) and (110) depict pure SiO<sub>2</sub> nanoparticles. Comparatively, it was noticed that the intensity of the peaks observed at 2θ value of 28.95° and 50.15 reduced with increasing concentration of NaOH. The suppression of the peaks may be linked to the Al<sub>2</sub>O<sub>3</sub> and NaOH. Conversely, low peak intensity and many other non-Quartz phases of SiO<sub>2</sub> nanoparticles such as Thenardite were observed in Figure 11. Similar trend was observed at pH 10 indicating poor quality of

SiO<sub>2</sub> nanoparticles produced. At 0.5M concentration of NaOH, SiO<sub>2</sub> nanoparticles produced from dealuminated metakaolin with Na<sub>2</sub>SiO<sub>3</sub> were comparable with the reference standard therefore indicating an optimum concentration for the production of SiO<sub>2</sub> from the two precursors. The further results revealed that peaks observed at all concentration of NaOH matched well to Quartz phase of SiO<sub>2</sub> nanoparticles and not all varied pH. The XRD characterization thus showed that the optimum condition in term of pH and concentration of NaOH for the production of SiO<sub>2</sub> produced from metakaolin with Na<sub>2</sub>SiO<sub>3</sub> were pH 5 and 0.5 M NaOH.

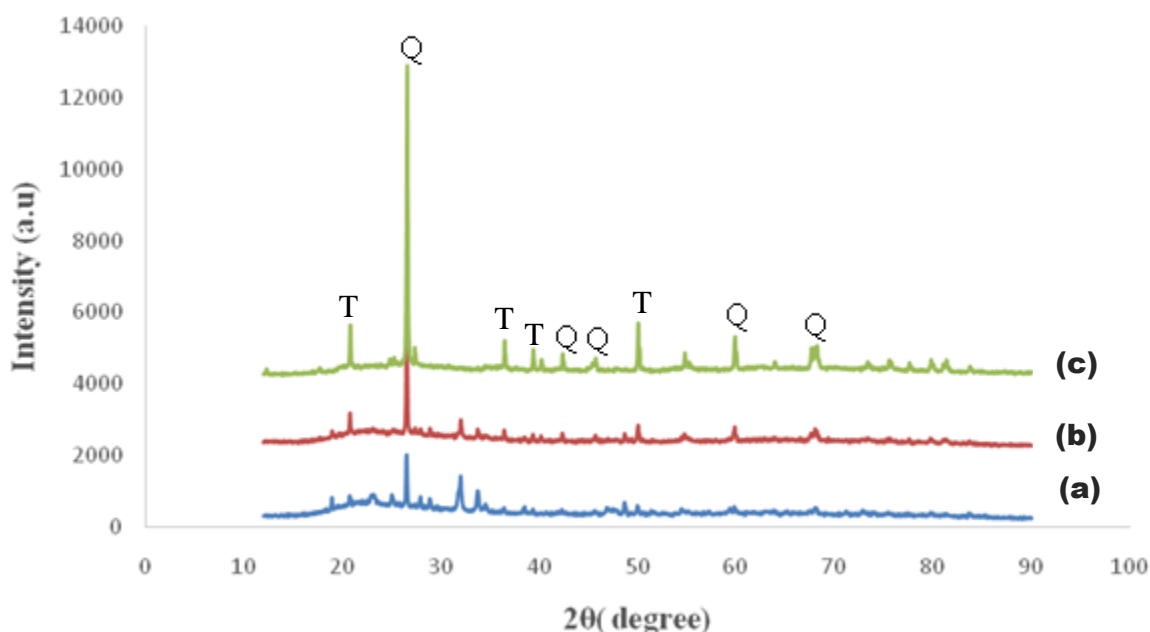


**Figure 11: X-ray Diffraction pattern of SiO<sub>2</sub> nanoparticles prepared from metakaolin with Na<sub>2</sub>SiO<sub>3</sub> at different solution pH (a) 5 (b) 8 (c) 10 (Where Q = Quartz, T = Thenardite)**

On the other hand, mixture of Thenardite and Quartz were observed at different diffraction angles when the solution pH of the mixture (Na<sub>2</sub>SiO<sub>3</sub> and metakaolin) was varied from 5, 8 – 10 (see Figure 11). This implies that formation of pure SiO<sub>2</sub> nanoparticles is not a function of pH but rather on concentration of NaOH. From

the observed peaks, intensity of the XRD diffractogram shown in Figure 11 increased with increasing pH, at pH 8, maximum peak and 2θ value were observed at 25.5° and 27.3° respectively. This matched almost with the standard reference peaks thus indicating an optimum pH for the production of Quartz phase

of SiO<sub>2</sub> nanoparticles from dealuminated metakaolin and Na<sub>2</sub>SiO<sub>3</sub>.

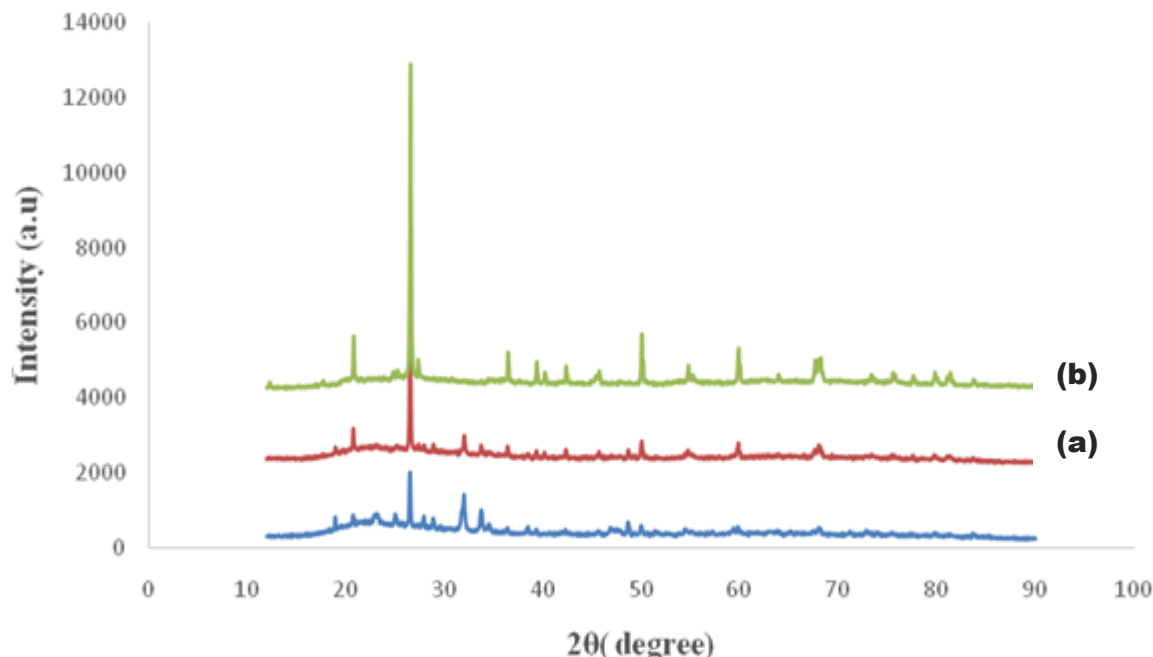


**Figure 12: X-ray Diffraction pattern of SiO<sub>2</sub> nanoparticles prepared from metakaolin mixed with Na<sub>2</sub>SiO<sub>3</sub> at different temperatures (a) 600°C (b) 700°C (c) 800°C Where; Q = Quartz**

In the same vein, pure SiO<sub>2</sub> nanoparticles were observed from mixture of Na<sub>2</sub>SiO<sub>3</sub> and dealuminated kaolin at different diffraction angles irrespective of the calcinations temperature (Figure 12). The finding in this study agreed with [10], who synthesized SiO<sub>2</sub> nanoparticles by Sol-Gel Process found Quartz phase SiO<sub>2</sub> only. Unlike Figure 10 and 11 where the peaks intensity were somewhat low, the diffraction peaks in Figure 11 were intense and sharp suggesting that the prepared SiO<sub>2</sub> nanoparticles are crystalline in nature.

### Conclusions

The aim of this research work was to investigate the optimum condition for the production of SiO<sub>2</sub> nanoparticle from dealuminated metakaolin and dealuminated metakaolin with Na<sub>2</sub>SiO<sub>3</sub> respectively. The analytical characterization results obtained from HRSEM, EDS and XRD confirmed that SiO<sub>2</sub> nanoparticle was synthesized. It was demonstrated that SiO<sub>2</sub>

nanoparticle obtained from dealuminated metakaolin under the influence of solution pH, calcinations temperature and concentration of NaOH is of high quality compared to others obtained from dealuminated metakaolin with Na<sub>2</sub>SiO<sub>3</sub>. The SiO<sub>2</sub> nanoparticles produced from dealuminated metakaolin contain the least impurities and can be used for biological application and easily dissolved in solvent. It was also demonstrated that crystalline SiO<sub>2</sub> nanoparticle produced at calcinations temperature of 700°C for dealuminated metakaolin, 700°C and 800°C dealuminated metakaolin with Na<sub>2</sub>SiO<sub>3</sub>, were highly crystalline compared to others at different synthesis conditions.

### Acknowledgements

The authors appreciate the contribution of the following people for their technical assistance: Dr. Remy Bucher (XRD analysis, ithemba Labs, South Africa); Dr. Franscious Cummings

(HRSEM/EDS analysis, Physics department, University of the Western Cape (UWC), South Africa). The authors acknowledged Tertiary Education Trust Fund, Nigeria, with grant number (TETFUND/FUTMINNA/2017/10) for the sponsorship.

## References

- [1]. N. Salahudeen, A.S. Ahmed, A.H Al-Muhtaseb, M. Dauda, S.M. Waziri, B.Y. Jibril, (2014). Synthesis and characterization of micro-sized silica from kankara kaolin. *Journal of Engineering Research*, 19(1), 235 – 241.
- [2]. B.J. Alloway, (2013). Sources of heavy metals and metalloids in soils. In *Heavy metals in soils* Springer, Dordrecht. 11-50. <http://www.springerlink.com/books>
- [3]. F. De Clippel, A. Harkiolakis, T. Vosch, X. Ke, L. Giebler, S. Oswald, P.A Jacobs (2011). Graphitic nanocrystals inside the pores of mesoporous silica: Synthesis, characterization and an adsorption study. *Microporous and Mesoporous Materials*, 144(1-3), 120-133.
- [4]. J.A. Harkless, D.K. Stillinger, F.H. Stillinger, (1996). Structures and energies of SiO<sub>2</sub> clusters. *The Journal of Physical Chemistry*, 100(4), 1098-1103.
- [5]. J. Sheng, K. Fan, D. Wang, C. Han, J. Fang, P. Gao, J. Ye (2014). Improvement of the SiO<sub>x</sub> passivation layer for high-efficiency Si/PEDOT: PSS heterojunction solar cells. *ACS Applied Materials & Interfaces*, 6(18), 16027-16034
- [6]. H. Fansuri, A. Iryani, W.E. Shahbihi, E. Santoso, D. Hartanto, R.M. Iqbal (2017). Effect of H<sub>2</sub>O/SiO<sub>2</sub> molar ratio on direct synthesis of ZSM-5 from Bangka's kaolin without pretreatment. *Malaysian Journal of Fundam Applied Science*, 13(4), 817-20.
- [7]. L. El Mir, A. Amlouk, C. Barthou, S. Alaya (2007). Synthesis and luminescence properties of ZnO/Zn<sub>2</sub>SiO<sub>4</sub>/SiO<sub>2</sub> composite based on nanosized zinc oxide-confined silica aerogels. *Physica B: Condensed Matter*, 388(1-2), 412-417
- [8]. V. Bansal, A. Ahmad, M. Sastry (2006). "Fungus-Mediated Biotransformation of Amorphous Silica Rice Husk to Nanocrystalline Silica". *Journal of the American Chemical Society*, 128(43): 14059-14066.
- [9]. G. Carturan, R. Campostrini, S. Dire, V. Scardi, E. De Alteriis, E (2004). Inorganic gels for immobilization of biocatalysts: inclusion of invertase-active whole cells of yeast (*Saccharomyces cerevisiae*) into thin layers of SiO<sub>2</sub> gel deposited on glass sheets. *Journal of Molecular Catalysis*, 57(1), L13-L16.
- [10]. R. Nandanwar, P. Singh, F.Z. Haque, (2015). Synthesis and Characterization of SiO<sub>2</sub> Nanoparticles by Sol-Gel Process and Its Degradation of Methylene Blue. *American Chemical Science Journal*, 5(1): 1-10.
- [11]. R. Peters, E. Kramer, A.G. Oomen, Z.E. Herrera Rivera, G. Oegema, P.C. Tromp, A.A. Peijnenburg (2012). Presence of nano-sized silica during in vitro digestion of foods containing silica as a food additive. *ACS Nano*, 6(3), 2441-2451.
- [12]. S. Mintova, M. Jaber, V. Valtchev (2015). Nano-sized microporous crystals: emerging applications. *Chemical Society Reviews*, 44(20), 7207-7233.
- [13]. A.O. Ajayi, A.Y. Atta, B.O. Aderemi, S.S. Adefila, (2010). "Novel Method of Metakaolin Dealumination - Preliminary Investigation". *Journal of Applied Sciences Research*, 6(10): 1539-1546.
- [14]. A.N. Haitao, J.N. Hasnidawania, H. Noritaa, S.N. Surip (2016). Synthesis of SiO<sub>2</sub> Nanostructures Using Sol-Gel Method. *Acta Physica Polonica A*, 129(4), 842 – 844.
- [15]. J. Gamelas, E. Ferraz, F. Rocha (2014). "An insight into the surface properties of calcined kaolinitic clays: the grinding effect". *Colloids and Surfaces A: Physicochemical and Engineering Aspects*. 455: 49–57.